



# True ternary fission, the collinear decay into fragments of similar size in the $^{252}\text{Cf}(\text{sf})$ and $^{235}\text{U}(\text{n}_{\text{th}}, \text{f})$ reactions



W. von Oertzen <sup>a,b,\*</sup>, A.K. Nasirov <sup>b,c</sup>

<sup>a</sup> Helmholtz-Zentrum Berlin, 14109 Berlin, Germany

<sup>b</sup> Joint Institute for Nuclear Research, 141980 Dubna, Russia

<sup>c</sup> Institute of Nuclear Physics, 100214, Tashkent, Uzbekistan

## ARTICLE INFO

### Article history:

Received 28 March 2014

Received in revised form 30 April 2014

Accepted 22 May 2014

Available online 28 May 2014

Editor: V. Metag

### Keywords:

Fission

Potential energy surfaces

Ternary fission

## ABSTRACT

The collinear cluster decay in  $^{252}\text{Cf}(\text{sf}, \text{fff})$ , with three cluster fragments of different masses (e.g.  $^{132}\text{Sn}$ ,  $^{52-48}\text{Ca}$ ,  $^{68-72}\text{Ni}$ ), which has been observed by the FOBOS group in JINR, has established a new decay mode of heavy nuclei, the collinear cluster tripartition (CCT). The same type of ternary fission decay has been observed in the reaction  $^{235}\text{U}(\text{n}_{\text{th}}, \text{fff})$ . This kind of “true ternary fission” of heavy nuclei has been predicted many times in theoretical works during the last decades. In the present note we discuss true ternary fission (TFFF) into three nuclei of almost equal size (e.g.  $Z = 98 \rightarrow Z_i = 32, 34, 32$ ) in the same systems. The possible fission channels are predicted from potential-energy (PES) calculations. These PES's show pronounced minima for several ternary fragmentation decays, e.g. for  $^{252}\text{Cf}(\text{sf})$  and for  $^{235}\text{U}(\text{n}_{\text{th}}, \text{f})$ . They suggest the existence of a variety of collinear ternary fission modes. The TFFF-decays chosen in this letter have very similar dynamical features as the previously observed collinear CCT-decays. The data obtained in the above mentioned experiments allow us to extract the yield for these TFFF-decays in both systems by using specific gates on the measured parameters. These yields are a few  $1.0 \cdot 10^{-6}$ /(binary fission).

© 2014 Published by Elsevier B.V. This is an open access article under the CC BY license (<http://creativecommons.org/licenses/by/3.0/>). Funded by SCOAP<sup>3</sup>.

## 1. Introduction

Binary fission has been studied intensively over the last four decades. For an overview there is the book edited by C. Wagemans: The Nuclear Fission Process [1], covering all important aspects of this process. A more recent theoretical coverage is available as a textbook by H. Krappe and Kr. Pomorski in Ref. [2]. Ternary fission, or light particle accompanied binary fission, has also been studied extensively. The name “ternary” fission has been used so far for such decays, when a third light particle is emitted *perpendicular* to the binary fission axis [3,4]. These previously studied ternary decays with lighter fragments, which are emitted from an oblate configuration, give decreasing yields as function of increasing mass(charge) of the third particle [4]. Recent experimental observations and numerous theoretical predictions [5–7,9] suggest, however, that in ternary decay the collinear configuration is preferred relative to the oblate configuration for heavy systems and ternary fragments with larger charge. The various manifestations

of this ternary decay mode studied in the recent years are now referred to as “true ternary fission”, e.g. Zagrebaev et al. in Ref. [10].

More recent surveys of clustering effects in fission and other binary decays can be found in articles (2010–2012) by G. Adamian, N. Antonenko and W. Scheid [11], and by D. Poenaru and W. Greiner [12]. An experiment to detect true ternary fission with three heavier fragments using detectors covering large ( $90^\circ$ ) angles to detect a *triangular shape of the decay-vectors* by Schall et al. [13] gave a negative result with a lower limit of  $1.0 \cdot 10^{-8}$ /(binary fission).

Ternary fission into fragments with comparable masses is a process, which occurs in heavy nuclei under conditions of large values of the fissility-parameter:  $X$ , for the ratios  $Z^2/A > 31$ . The decay into three heavier fragments (true ternary fission) observed is found to be collinear, as in fact often predicted in the last decades [5–7,9]. Recent experiments of two fragment coincidences with two FOBOS-detectors [14] placed at  $180^\circ$ , using the missing mass approach have established the phenomenon of *collinear cluster tripartition*, the CCT-decay. This new decay mode has been observed for the spontaneous decay of  $^{252}\text{Cf}(\text{sf}, \text{fff})$  and for neutron induced fission in  $^{235}\text{U}(\text{n}_{\text{th}}, \text{fff})$ , see Refs. [14–16]. In this fission mode, the CCT, with the emission of three fragments, the outer fragments of the “chain” are registered [14]. Here typical fragments

\* Corresponding author at: Helmholtz-Zentrum Berlin, 14109 Berlin, Germany.

E-mail addresses: [oertzen@helmholtz-berlin.de](mailto:oertzen@helmholtz-berlin.de) (W. von Oertzen), [nasirov@jinr.ru](mailto:nasirov@jinr.ru) (A.K. Nasirov).

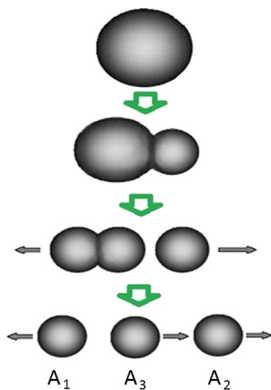


**Fig. 1.** Schematic illustration of collinear sequential ternary fission into three fragments of comparable mass.

are isotopes (clusters, nuclei with closed shells) of Sn, Ni, and Ca. The latter, Ca, as the smallest third particle is positioned along the line connecting Sn and Ni, in this way minimizing the potential energy. In the experiments described in Refs. [14,15], two of the three fragments, emitted in one direction, moving towards one of the detectors (called arm1) are dispersed in angle in the source backing. Due to this angular dispersion one of them is lost on a structure in front of the detectors. Thus binary coincidences are obtained with the missing mass method (e.g.  $A_3 = 48\text{--}52$ , missing Ca isotopes). This new exotic decay can be understood as the breakup of very (prolate deformed) elongated hyper-deformed shapes, see Ref. [17] for a discussion of hyper-deformation in  $^{236}\text{U}$ . The decay is considered with two sequential neck ruptures [16,18], as illustrated in Fig. 1.

From the recent work on CCT-decays and in a survey of the theoretical predictions of the last decades, see Ref. [16], it became clear, that for larger charge (mass) of the third central fragment,  $A_3 > 40$ , the ternary decay must be collinear. The collinear aligned multi-cluster configurations are energetically the optimal configurations for ternary decays [6,7,9].

In the work presented here we use the potential energy surfaces, PES (as defined in Ref. [19]), to discuss the relative importance of different ternary fission modes. The PES are defined as the energy balance in the sum of interactions (nuclear and Coulomb) between all three fragments and the ground state energy (masses) balance of all three fragments, the  $Q_{\text{ggg}}$ -values. The latter is determined by the balance of the binding energies of the three fragments and the decaying nucleus (with the masses taken from Moeller and Nix [8]). The results of the calculations are shown as contour-plots in Fig. 2. Further details of the presently used advanced version of the method used in Ref. [19] will be given in a next publication [23]. Considering the phase space (see below) for the decays, we can observe several favored regions for ternary fission, defining several ternary decay modes. From these results we conclude, that for the CCT-decay in  $^{252}\text{Cf}(\text{sf}, \text{fff})$ , the arrangement with Ca as a third fragment in the center gives a lower value of the potential energy. More explicitly: the arrangement of the charges with  $(Z = 28, 20, 50)$  is favored in the ternary decay relative to  $(Z = 20, 28, 50)$  by an energy difference of about 10 MeV, as observed in Ref. [14].

We will study (true) ternary fission decays predicted by the PES's, with *almost equal fragment masses*, with  $A_1 \approx A_2$ ,  $A_3 \approx A_2$ , which we will call TFFF. Within the three-cluster model it has been shown [9], that for ternary decays of heavy nuclei, the collinear configuration is favored and that for masses (charges) of central clusters heavier than  $A_3 = 35\text{--}40$  the prolate fission starts to dominate. For the true ternary fission (TFFF) considered here, with almost equal masses of the fragments  $A_1$ ,  $A_2$ ,  $A_3$ , collinear ternary

fission will dominate over oblate fission by more than 5 orders of magnitude as predicted in Ref. [9]. This fact is due to the dominant Coulomb interaction, which is minimized for the collinear configurations. The dark blue regions on the right lower corner in the contour-plots of Fig. 2 correspond to collinear ternary fission with light fragments  $Z_3$  will be discussed in the next publication.

## 2. Potential energy surface (PES) and ternary fission

In order to judge the relative importance of different ternary fission modes, the potential energy surfaces, PES's, have been calculated by Nasirov et al. [19,20] for the ternary decays of  $^{236}\text{U}^*$  and of  $^{252}\text{Cf}(\text{sf}, \text{fff})$ . The PES will dominantly determine the available phase space, and thus the yields. The result will be complemented by an evaluation of the internal barriers of the sequential decays as discussed by Nasirov et al. [20].

From the experiments reported in Refs. [14,15] on CCT for  $^{252}\text{Cf}(\text{sf}, \text{fff})$  and  $^{235}\text{U}(\text{n}_{\text{th}}, \text{fff})$  an overall yield of  $4 \cdot 10^{-3}$ /(binary fission), contained in a larger bump of fragment mass combinations has been observed. This result has been considered to have unusually high values, when compared with the previously known yields in “ternary fission” with the emission of one isotope of lighter fragments perpendicular to the fission axis [3,4]. The observation of CCT with high probability can be explained if the *phase space* for the statistical fission process is considered, see in particular Refs. [16,18]. The phase space of statistical decay depends on:

- i) the details of the PES, namely, the geometrical size of its valleys and hills,
- ii) the  $Q_{\text{ggg}}$ -values, the latter determining the number of possible fragment (isotope) combinations,
- iii) the excitation energy range in the individual fragments,
- iv) the momentum range,
- v) the number of excited states (density of states) in each of the fragments, the combinations consisting of 2(3) isotopes, and
- vi) the spin ( $J$ ) multiplicity in these states with spins up to  $(6\text{--}8)^+$  (phase space factor  $(2J + 1)$ ).

For the ternary decays of  $^{252}\text{Cf}$ , the PES's, contour-plot in Fig. 2, show distinct minima for various charge combinations with  $\Sigma Z = 98$ :

- i) for CCT  $Z_3 = 20$ , and  $Z_1 = 28$  and
- ii) less pronounced for  $Z_3 = 28$ , and  $Z_1 = 20$ . The complementary fragments with  $Z_2$  are isotopes of Sn ( $Z = 50$ ). In addition we observe a pronounced region of minima for the charge combinations with three comparable fragments, for the TFFF-decays:
- iii)  $(Z_1 = 32, 34, 32)$ ,  $Z_3 = (34, 32, 30)$ , the fragment  $Z_2$  has an equivalent role and  $Z$ -values  $Z_2 = 32, 34$ , similar to the first two values of  $Z_1, Z_3$  – we have an almost symmetric ternary decay. Because of this fact, permutations of the labels including  $Z_2$  in the PES (contour plots in Fig. 2) will produce similar results, and a symmetric shape of the data in the favored region (by reflection of the labels). For the experimental data, we have the possibility to select events with the conditions on the velocities  $V_3 \approx V_2$  and  $V_3 \approx V_1$ , for a symmetric decay, see Fig. 3. This choice reduces completely the background due to the scattering tails and other ternary decay modes in the data. Because of the symmetry discussed before the events appear as a rectangular region, which corresponds to the true ternary fission into three equivalent fragments, (TFFF), as predicted by the PES's, Fig. 2.

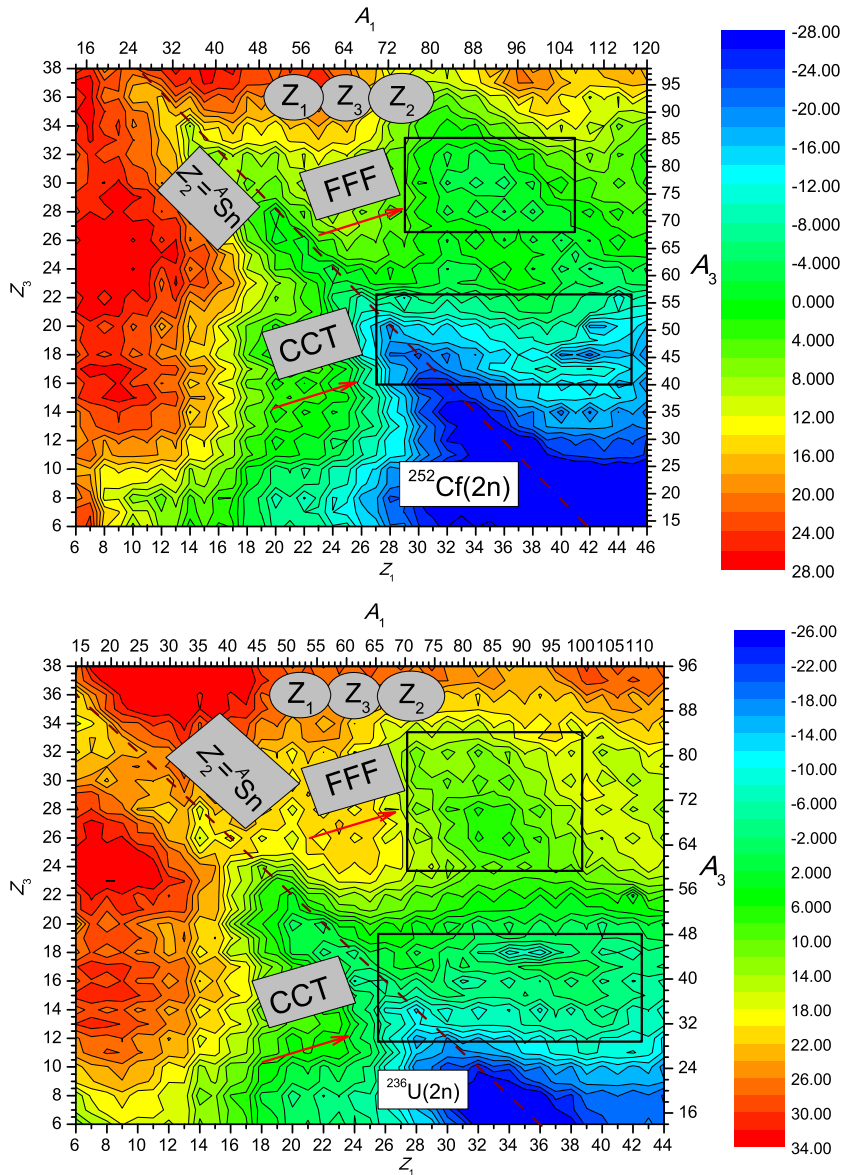


**Fig. 2.** (Color online.) The contour plots of the potential energy surfaces (PES) for the ternary decays characterized by fragments  $Z_3$  and  $Z_1$ . i) (upper part) for  $^{252}\text{Cf}$  and ii), (lower part), for  $^{236}\text{U}^*$ , respectively. The fragments with  $Z_2$  can be typically the isotopes of tin,  $^{128-132}_{50}\text{Sn}$ , labeled according to the inserts.

Inspecting the contour-plots of the PES-calculations for  $^{236}\text{U}$  ( $Z = 92$ ), shown in the lower part of Fig. 2, we see minima for the values ( $Z_3 = 24-28$ , and  $Z_1 = 32, 34$ ), with the corresponding values of ( $Z_2 = 32, 34$ ), indicating the population of an asymmetric distribution (now with a smaller sum of charges,  $\sum_{i=1}^3 Z_i = 92$ ). In the correlation plot for  $A_1-A_3$  events forming a right angle are predicted. The shape of the favored region is less symmetric as compared to the case of  $^{252}\text{Cf}$ . In the experimental data a selection of TFFF decays with almost equal momenta/velocities is achieved by selecting the velocities and the momenta, with  $V_1 \approx V_2$ . The TFFF-decays form two branches, which are positioned at a right angle. The experimental result is shown in Fig. 5, we observe a distinct concentration for events with  $A_1 = 70-82$  in coincidence with  $A_3 = 68-72$ , and vice versa  $A_1 = 66-72$ , and (the missing mass  $A_2 = 68-90$ ), the binary sum being  $\sum(A_1 + A_2) = (140-144)$ . This experimental yield is determined by combinations of charges, with the corresponding masses. Note that in the experiments binary, ( $A_1$  and  $A_2$ ), coincidences are registered with the two “outer” fragments, with a missing mass labelled  $A_3$ . This arrangement

is used in the illustration of the contour-plots of the PES's in Fig. 2. This approach selects the TFFF-decay, and reduces very efficiently the background. Two branches as predicted by the PES's are observed. These cannot be observed in the inclusive data from Ref. [14], shown in Fig. 4. These data show the large background due to scattering on the detector frames and due to various other ternary decay modes. The arrow shows the region of the original CCT mode as described in Ref. [14], and there are events with mass combinations of ternary decays, which will be analyzed later.

For the purpose of calculating the PES it is useful to cite results of an experiment reported in Ref. [21] on the  $^{235}\text{U}(n_{\text{th}}, \text{ff})$  reaction with coincidences of fragments with  $\gamma$ -emissions. From this work we deduce that the maximum neutron emission probability is typically in the 2n- and 3n-channels. In our case two neck ruptures may produce two neutrons from scission at each event. Therefore the PES in Fig. 2, were calculated for the 2n-channel. In this work also the average spin values in the fission fragments has been obtained, spins up to values of  $8^+$  are observed. We may assume, that similar values appear in ternary fission, in the TFFF-decays.

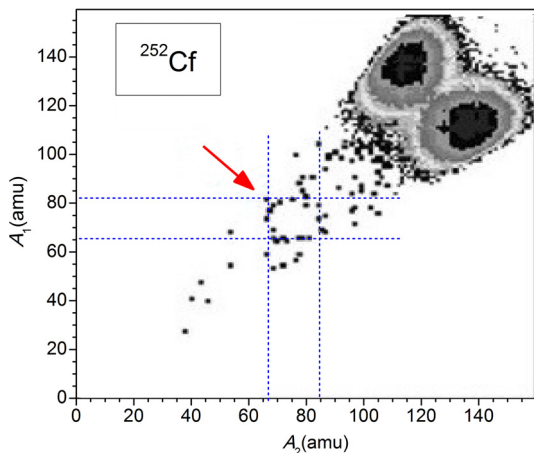


**Fig. 3.** Binary coincidences of fragments in the spontaneous decay of  $^{252}\text{Cf}(\text{sf})$  from the data measured in Ref. [14]. There the outer fragments ( $A_1, A_2$ ) are registered. For the selection of TFFF decays, a gate on the condition ( $V_1 \approx V_2$ , and  $P_1 \approx P_2$ ) is chosen. Remnants of the binary fragments coincidences are seen. The region favored for the TFFF-decay is marked. Missing fragments ( $A_3$ ) here are isotopes of nuclei with ( $Z_3 = 30\text{--}36$ ). Points above this region are other symmetric ternary decays.

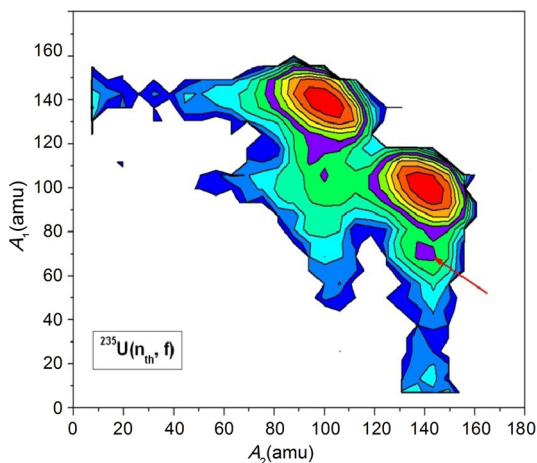


**Fig. 4.** (Color online.) Binary inclusive coincidences of fragments in the reaction  $^{235}\text{U}(\text{n}, \text{fff})$  as measured and published in Ref. [14]. The position of the missing mass peak,  $A_3$ , in CCT-decay is marked by an arrow. Missing fragments for TFFF here are isotopes of ( $Z_3 = 30\text{--}36$ ). The general structure of the coincidence events is very similar to  $^{252}\text{Cf}(\text{sf}, \text{fff})$ , see Refs. [14] for details.

For the CCT-decay of  $^{252}\text{Cf}(\text{sf}, \text{fff})$  the PES shows, that we have favorable dynamical conditions for the sum of fragments with mass combinations of clusters:  $^{60\text{--}70}\text{Ni}$  with  $^{130\text{--}134}\text{Sn}$ , and with missing  $^{50\text{--}58}\text{Ca}$  (as reported in Ref. [14]). For this channel the total phase space (discussed also in Ref. [18]) is factors of 3000–10000 larger, compared to the phase space in the “ternary fission” with particular mass combinations [3], decays with one light particle without excited states emitted. With the large  $Q$ -values of these mass partitions (e.g. 251.37 MeV, for  $^{132}\text{Sn} + ^{50}\text{Ca} + ^{70}\text{Ni}$ ) in CCT events, many fragment combinations are formed like in the bumps observed in binary fission. The phase space is discussed in a study of the kinematics for the collinear breakup into isotopes of (Sn + Ca + Ni) in Ref. [18]. In this study the assumption of a sequential decay is made corresponding to two neck ruptures. These neck configurations are connected to the concept of hyper-deformation, see Ref. [17]. The same assumptions apply to the TFFF-decays (as suggested in Fig. 1), the time sequence of the two random (in time) neck-ruptures is connected to the binary fission times. In fact proceeding for TFFF-decays as in Ref. [18], to calculate the kinetic energies of the central fragment, we find that

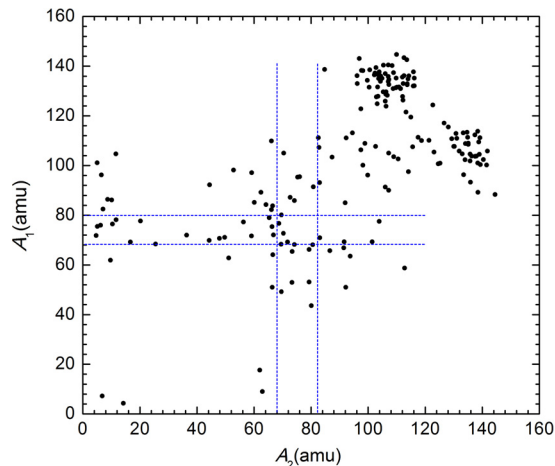


**Fig. 5.** (Color online.) The distribution of events with coincident fission fragments from the decay of  $^{236}\text{U}^*$  (7 MeV), selected with the conditions on velocities and momenta, ( $V_1 \approx V_2$ , and  $P_1 \approx P_2$ ). The lines show the expected borders for two fragment coincidences with masses (68–82).

the kinetic energy of the central fragment in TFFF-decay will have values close to zero! Therefore, in the TFFF-decay the central fragment will be stopped in the target or/and in the backing pointing to arm 1, leading to binary coincidences with a missing mass of  $A_3 = 70\text{--}80$ .

From the considerations elaborated above, we expect true TFFF-decays with (e.g.  $Z_3 = 32$ ,  $Z_1 = 34$ , and  $Z_2 = 32$ , for  $^{252}\text{Cf}(\text{sf})$ ), they are collinear and that the fragments in the middle ( $Z_3$ ) can not be observed. Clearly some deformation effects play a role, also the fact that we have three fragments with binding energies close to the maximum of the of the overall values of the (binding energy)/nucleon, resulting in larger  $Q$ -values and deeper holes in the PES's. The  $Q$ -value for the TFFF-decay in  $^{252}\text{Cf}(\text{sf}, \text{FFF})$  is  $Q_{\text{TFFF}} = 268.3$  MeV, it is larger then for CCT ( $Q_{\text{CCT}} = 250.6$  MeV) and binary decays (205 MeV).

However, we expect a much smaller total probability for TFFF-decays compared to the CCT-decay. From the events attributed to the TFFF decay shown in Fig. 5 we obtain an overall probability of  $4.0 \cdot 10^{-6}/(\text{binary fission})$ , namely approx. 100–1000 times smaller then observed for the CCT decay, of ( $4.1 \cdot 10^{-3}$ ), as cited in Ref. [14].

The PES for  $^{252}\text{Cf}(\text{sf}, \text{FFF})$  suggests other ternary decay modes, we see an additional pronounced minimum for charge combinations with  $Z_3 = 18$ , and  $Z_1 = 42$ , (for masses 44 (Ar) and 104 + 104 (Mo)). A strong yield of fragment combinations is expected. This is in fact observed as a peak with  $A = 104$  in Fig. 6.11 of the recent survey by Pyatkov and Kamanin in Ref. [22] on the experimental results on fission studies with the particular set-up of Ref. [14]. A special method is described there, this will be analyzed in a future publication [23]. For  $^{235}\text{U}(\text{n}_{\text{th}}, \text{fff})$ , the corresponding experimental result as a subset of the data with the conditions  $V_1 \approx V_2$ , ( $\pm 10\%$ ) and  $P_1 \approx P_2$ , were obtained, shown in Fig. 5. In this experimental binary mass ( $A_1, A_2$ )-coincidence plot, the missing mass is seen with the two masses around  $\sum_{i=1,2} = 150\text{--}160$ , this corresponds to a missing mass  $A_3 = 86\text{--}76$ . Other ternary decay modes expected from the PES-landscape (lower right corner) will be treated in the next publication [23].

We conclude that in the data of Refs. [14,15] several kinds of collinear ternary fission modes must be contained, the original CCT-decay from Ref. [14], and the symmetric TFFF-decay presented here. In the TFFF-case the third central fragment has comparable mass with the other two, and has extremely low kinetic energy, therefore it is usually stopped in the target and/or in the backing.

The observations presented here, point to the fact, that true ternary fission encompasses a larger variety of collinear fission modes, these are suggested by the PES-calculations. We have shown that the TFFF-mode, with three almost equal mass fragments is observed simultaneously with the more asymmetric CCT-events reported earlier in Ref. [14].

### Acknowledgements

We thank our colleagues, Y. Pyatkov and D. Kamanin for their important discussions and for providing us with the data shown in the Figs. 3 and 5. A.K.N. is grateful to RFBR for partial support. W.v.O. thanks the FLNR of JINR for their hospitality extended to him during his stays in Dubna.

### References

- [1] C. Wagemans (Ed.), *The Nuclear Fission Process*, CRC Press Inc., 1991.
- [2] H. Krappe, Kr. Pomorski, *Theory of Nuclear Fission: A Textbook*, *Lect. Notes Phys.*, vol. 838, Springer-Verlag, Heidelberg, 2012.
- [3] F. Gönnerwein, *Nucl. Phys. A* 734 (2004) 213.
- [4] F. Gönnerwein, *Europhys. News* 36 (1) (2005) 11.
- [5] H. Diehl, W. Greiner, *Nucl. Phys. A* 229 (1974) 29.
- [6] D.N. Poenaru, R.A. Gherghescu, W. Greiner, *Nucl. Phys. A* 747 (2005) 182–205.
- [7] G. Royer, *J. Phys. G, Nucl. Part. Phys.* 21 (1995) 249.
- [8] P. Moeller, J.R. Nix, W.D. Meyers, W.J. Swiatecki, *At. Data Nucl. Data Tables* 59 (1995) 185.
- [9] K. Manimaran, et al., *Phys. Rev. C* 83 (2011), 034609.
- [10] V.I. Zagrebaev, A.V. Karpov, W. Greiner, *Phys. Rev. C* 81 (2010), 044608; Also V. Zagrebaev, W. Greiner, in: C. Beck (Ed.), *Clusters in Nuclei*, vol. 1, in: *Lect. Notes Phys.*, vol. 818, Springer-Verlag, Heidelberg, Berlin, 2010, pp. 267–315, Chapter 7.
- [11] G. Adamian, N. Antonenko, W. Scheid, in: C. Beck (Ed.), *Clusters in Nuclei*, vol. 2, in: *Lect. Notes Phys.*, vol. 848, Springer-Verlag, Heidelberg, Berlin, 2012, pp. 165–227.
- [12] D. Poenaru, W. Greiner, in: C. Beck (Ed.), *Clusters in Nuclei*, vol. 1, in: *Lect. Notes Phys.*, vol. 875, Springer-Verlag, Berlin, Heidelberg, 2010, pp. 1–56.
- [13] P. Schall, et al., *Phys. Lett. B* 191 (1987) 339.
- [14] Yu.V. Pyatkov, et al., *Eur. Phys. J. A* 45 (2010) 29.
- [15] Yu.V. Pyatkov, et al., *Eur. Phys. J. A* 48 (2012) 94.
- [16] W. von Oertzen, Y.V. Pyatkov, D. Kamanin, in: *Zakopane Conference*, *Acta Phys. Pol.* 44 (2013) 447.
- [17] M. Csatlos, A. Krasnahorkay, P.G. Thirolf, et al., *Phys. Lett. B* 615 (2005) 213.
- [18] K.R. Vijayaraghavan, W. von Oertzen, M. Balasubramaniam, *Eur. Phys. J. A* 48 (2012) 27.
- [19] R.B. Tashkodajev, A.K. Nasirov, W. Scheid, *Eur. Phys. J. A* 47 (2011) 136.
- [20] A. Nasirov, et al., *Phys. Scr.* 89 (2014) 054022.
- [21] S. Mukhopadhyay, et al., *Phys. Rev. C* 85 (2012), 064321.
- [22] D. Kamanin, Y.V. Pyatkov, in: C. Beck (Ed.), *Clusters in Nuclei*, vol. 3, in: *Lect. Notes Phys.*, vol. 875, Springer, Heidelberg, Berlin, 2014, pp. 183–246, Chapter 6.
- [23] A. Nazirov, W. von Oertzen, D. Kamanin, Y.V. Pyatkov, unpublished, submitted for publication, 2014.